J|A|C|S COMMUNICATIONS

Published on Web 04/08/2009

Characterization of a Peroxodiiron(III) Intermediate in the T201S Variant of Toluene/*o*-Xylene Monooxygenase Hydroxylase from *Pseudomonas* sp. OX1

Woon Ju Song,[†] Rachel K. Behan,[†] Sunil G. Naik,[‡] Boi Hanh Huynh,*[,‡] and Stephen J. Lippard*[,†]

Department of Chemistry, Massachusetts Institute of Technology, Cambridge, Massachusetts 02139, and Department of Physics, Emory University, Atlanta, Georgia 30322

Received February 14, 2009; E-mail: lippard@mit.edu; vhuynh@physics.emory.edu

Carboxylate-bridged diiron centers are common active-site motifs in enzymes, performing a variety of dioxygen-dependent functions, including hydrocarbon oxidation.[1−4] The diiron centers in these enzymes have similar primary coordination spheres,[5−7] suggesting that the protein scaffold tunes their chemical reactivity to favor a specific reaction pathway. Previous construction of variants of RNR-R2[8] and ToMOH demonstrated that changes in the secondary and tertiary coordination spheres can divert the reaction pathway from electron abstraction to aromatic hydroxylation and vice versa.[9,10] For these variants, however, the chemistry of the diiron(II) cluster with dioxygen was unchanged, and the oxygenated intermediates reacted with nearby amino acid residues. Here, we provide the first direct evidence that a single conservative amino acid mutation in BMMs can partially bifurcate the oxygenation reaction to generate a diiron(III) peroxo intermediate not observed in the native system.

Recently, a transient diiron(III) intermediate in ToMOH, $ToMOH_{peroxo}$, was identified by Mössbauer spectroscopy and shown to be kinetically competent for arene oxidation.[11] Although this enzyme is similar to sMMOH in both sequence[12] and active-site structure,[13] the spectroscopic properties of $ToMOH_{peroxo}$ were unexpected. Whereas H_{peroxo} in sMMOH displays an optical band at ~720 nm (ε_{720} = ~2000 cm^{-1} M^{-1})[14,15] and exhibits Mössbauer parameters of $\delta = 0.66$ mm/s and $\Delta E_Q = 1.51$ mm/s,[16] $ToMOH_{peroxo}$ has no optical bands in the visible region and Mössbauer parameters of $\delta = 0.54$ mm/s and $\Delta E_Q = 0.67$ mm/s.[11] No other transient intermediate, like Q, was observed in ToMOH. These results suggest that $ToMOH_{peroxo}$ has a structure distinct from that of any other peroxodiiron(III) intermediate in carboxylate-bridged diiron proteins, including sMMOH, Δ9D,[17] and RNR-R2 variants.[18,19]

The T201S variant in ToMOH (hereafter T201S) was originally prepared to investigate the role of a strictly conserved threonine residue near the carboxylate-bridged diiron active site on catalysis.[13] During the course of our study, a structure of the T4moHD complex was reported revealing T201 to be involved in a novel hydrogen-bonding network terminating at a water molecule coordinated to Fe1.[20] The steady-state activity for conversion of phenol to catechol in T201S was measured to be 2400 ± 300 mU/mg (mU = nmol/min), compared to that of wild-type enzyme, 1200 ± 200 mU/mg, respectively.[21] This result indicates that T201S is even more efficient than wild-type enzyme in aromatic hydroxylation. A Michaelis−Menten kinetic analysis revealed k_{cat} and k_{cat}/K_M values for T201S of 0.08 ± 0.03 s^{-1} and 0.02 μM^{-1} s^{-1}, respectively, which are not greatly different from those of the wild-type enzyme, 0.049 ± 0.003 s^{-1} and 0.011 ± 0.003 μM^{-1} s^{-1}. The T201S variant produced the same product yield as wild-type enzyme for phenol oxidation, corresponding to ~50% of the diiron sites in a single-turnover reaction of reduced diiron(II) ToMOH with O_2.[22] The regiospecificity of T201S for toluene hydroxylation was also conserved at a 3:2:5 ratio of *o*:*m*:*p*-cresol, and that for *o*-xylene hydroxylation was slightly perturbed in T201S, changing the ratio of the two products from 2:8 to 4:6 2,3-dimethylphenol vs 3,4-dimethylphenol.[23]

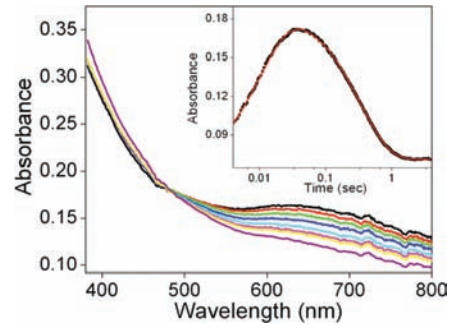

Figure 1. UV−vis spectrum of the reaction of reduced ToMOH T201S in the presence of ToMOD mixed with dioxygen-saturated buffer. [ToMOH] = ~120 μM, [ToMOD] = 360 μM in 25 mM MOPS, pH 7.0 at 4.0 ± 0.1 °C. (Inset) Time-dependent absorption trace monitored at 675 nm, shown with the fit.

When investigating pre-steady-state dioxygen activation at the reduced diiron(II) center of T201S by stopped-flow spectrophotometry, we observed a new transient intermediate ($T201S_{peroxo}$) with a broad absorption band at λ_{max} ~ 650 nm (Figure 1 and Supporting Information, Figure S1) and $\Delta\lambda$ ~ 700 nm (Supporting Information, Figure S2). This feature provides optical spectroscopic evidence for an oxygenated intermediate in toluene monooxygenase. A typical kinetic trace of the growth and decay of the transient intermediate is provided in the inset of Figure 1, together with the fit. The absorbance at 675 nm maximizes at ~40 ms after dioxygen is mixed at 4.0 ± 0.1 °C. Fitting the time-dependent absorption spectra to a $ToMOH_{red}$ → $T201S_{peroxo}$ → diiron(III) product model yielded $k_{form} = 85 \pm 11$ s^{-1} and $k_{decay} = 2.9 \pm 0.2$ s^{-1}. The intermediate is observed only in the presence of the regulatory protein (ToMOD), which is consistent with previous reports on oxygenated intermediates in BMMs such as H_{peroxo} or Q in sMMOH,[24] or $ToMOH_{peroxo}$ in wild-type[11] or I100W ToMOH.[25]

To investigate further the spectroscopic properties of this intermediate, we performed Mössbauer studies with ^{57}Fe-enriched T201S ToMOH enzyme. We present the Mössbauer spectra of reduced diiron(II) in the presence of ToMOD (Figure 2A), a rapid freeze-quenched sample at 45 ms (Figure 2B), and the diiron(III) product (Figure 2C). The spectra corresponding to the diiron(II) starting material and diiron(III) product of T201S ToMOH were respectively fit to (i) two quadrupole doublets having the same $\delta = 1.32$ mm/s, ΔE_Q = 2.32 and 3.16 mm/s and (ii) $\delta = 0.50$ mm/s, $\Delta E_Q = 0.82$. Within experimental error, these parameters are indistinguishable from those of wild-type ToMOH. When T201S $ToMOH_{red}$ was allowed to react with dioxygen (Figure 2B), we observed that only 50% of the diiron(II)

[†] Massachusetts Institute of Technology.
[‡] Emory University.

10.1021/ja9011782 CCC: $40.75

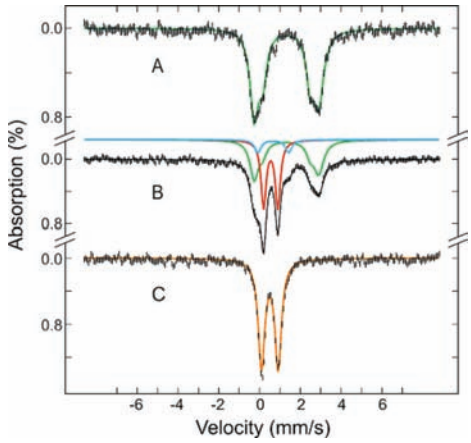

Figure 2. Mössbauer spectra of freeze-quenched samples from reaction of $ToMOH_{red}$T201S:3ToMOD with O_2. The spectra (vertical bars) are collected at 4.2 K in a 50-mT field parallel to the γ-beam. The three spectra correspond to (A) the diiron(II) starting material, (B) the sample 45 ms after mixing with O_2, and (C) the diiron(III) product. The green, red, cyan, and orange lines are simulated spectra of the unreacted diiron(II) protein, $ToMOH_{peroxo}$, $T201S_{peroxo}$, and diiron(III) product, respectively. The solid line overlaid with the experimental spectrum in panel B is the composite spectrum.

sites react, whereas the rest become slowly oxidized to a diiron(III) species, suggesting half-sites reactivity as in wild-type ToMOH and the small subunit of ribonucleotide reductase.[11,26]

Upon reaction of T201S $ToMOH_{red}$ with dioxygen in the presence of ToMOD, two distinctive transient intermediates accumulate (Figure 2B). One of the intermediates displays Mössbauer parameters very similar to those of the diiron(III) intermediate in wild-type ToMOH, with $\delta = 0.55$ mm/s and $\Delta E_Q = 0.70$ mm/s. This intermediate, $ToMOH_{peroxo}$, accounts for approximately 40% of total iron at 45 ms and fully decays by ~100 s (Figure 2C), exhibiting kinetic behavior similar to that of $ToMOH_{peroxo}$ in the wild-type enzyme. As in the wild type, $ToMOH_{peroxo}$ generated in T201S also has no optical band in the visible range.

The other intermediate displays Mössbauer parameters identical to those of H_{peroxo} in sMMOH with $\delta = 0.67$ mm/s and $\Delta E_Q = 1.51$ mm/s, implying that the structure of $T201S_{peroxo}$ is similar to the structure of H_{peroxo} in sMMOH, but different from that of $ToMOH_{peroxo}$. This intermediate accounts for 10% of the total iron in the Mössbauer spectrum of the sample (Figure 2B), which allows us to estimate the molar extinction coefficient of $T201S_{peroxo}$ to be $\varepsilon_{675} \sim 1500$ cm^{-1} M^{-1}. This value is within the range of those reported for peroxo-to-iron charge-transfer bands in several diiron(III) peroxo enzyme intermediates[14,15,17,18,27] as well as synthetic model complexes.[28,29] Given these spectroscopic similarities, we assign this species as a peroxodiiron(III) intermediate. Moreover, the kinetic properties of the two discrete diiron(III) intermediates demonstrate that $T201S_{peroxo}$ is neither a precursor nor a successor of $ToMOH_{peroxo}$, for which $k_{form} \sim 26$ s^{-1}, implying that T201S has an additional, alternative pathway of activating dioxygen.

In conclusion, an oxygenated intermediate having an optical band in ToMOH is generated by a single, conservative mutation of the T201 residue. Although during dioxygen activation T201S generates $T201S_{peroxo}$ and $ToMOH_{peroxo}$, the former being similar to $MMOH_{peroxo}$, it behaves in a manner similar to the wild-type enzyme in steady-state activity and single-turnover experiments. It also has regiospecificity comparable to that of the wild-type enzyme in toluene and *o*-xylene oxidations. Time-resolved optical and rapid freeze-quench Mössabuer experiments strongly support the assignment of the oxygenated intermediate in ToMOH, $T201S_{peroxo}$, as a peroxodiiron(III) species. Although further studies are required to define the mechanism of dioxygen activation and the role of the T201 residue in ToMOH, our results raise the interesting possibility that this single amino acid perturbs the thermodynamics of dioxygen activation in carboxylate-bridged non-heme diiron BMM enzymes.

Acknowledgment. This work was supported by grants GM32134 (to S.J.L.) and GM 47295 (to B.H.H.) from the National Institute of General Medical Sciences. R.K.B. acknowledges fellowship support from the NIGMS (1 F32 GM084564-01). We thank Prof. J. Stubbe for use of her freeze-quench apparatus and Dr. L. J. Murray for helpful comments on the manuscript.

Supporting Information Available: Experimental details. This material is available free of charge via the Internet at http://pubs.acs.org.

References

(1) Merkx, M.; Kopp, D. A.; Sazinsky, M. H.; Blazyk, J. L.; Müller, J.; Lippard, S. J. *Angew. Chem., Int. Ed.* **2001**, *40*, 2782–2807.
(2) Wallar, B. J.; Lipscomb, J. D. *Chem. Rev.* **1996**, *96*, 2625–2657.
(3) Stenkamp, R. E. *Chem. Rev.* **1994**, *94*, 715–726.
(4) Stubbe, J.; Nocera, D. G.; Yee, C. S.; Chang, M. C. Y. *Chem. Rev.* **2003**, *103*, 2167–2202.
(5) Rosenzweig, A. C.; Frederick, C. A.; Lippard, S. J.; Nordlund, P. *Nature (London)* **1993**, *366*, 537–543.
(6) Holmes, M. A.; Le Trong, I.; Turley, S.; Sieker, L. C.; Stenkamp, R. E. *J. Mol. Biol.* **1991**, *218*, 583–593.
(7) Nordlund, P.; Eklund, H. *J. Mol. Biol.* **1993**, *232*, 123–164.
(8) Abbreviations: RNR-R2, *E. coli* ribonucleotide reductase R2 subunit; ToMO, toluene/*o*-xylene monooxygenase; MMOH, methane monooxygenase hydroxylase; BMM, bacterial multicomponent monooxygenase; Δ9D, Δ^9-desaturase; T4moH, toluene 4-monooxygenase hydroxylase.
(9) Baldwin, J.; Voegtli, W. C.; Khidekel, N.; Moënne-Loccoz, P.; Krebs, C.; Pereira, A. S.; Ley, B. A.; Huynh, B. H.; Loehr, T. M.; Riggs-Gelasco, P. J.; Rosenzweig, A. C.; Bollinger, J. M., Jr. *J. Am. Chem. Soc.* **2001**, *123*, 7017–7030.
(10) Murray, L. J.; García-Serres, R.; McCormick, M. S.; Davydov, R.; Naik, S. G.; Kim, S.-H.; Hoffman, B. M.; Huynh, B. H.; Lippard, S. J. *Biochemistry* **2007**, *46*, 14795–14809.
(11) Murray, L. J.; Naik, S. G.; Ortillo, D. O.; García-Serres, R.; Lee, J. K.; Huynh, B. H.; Lippard, S. J. *J. Am. Chem. Soc.* **2007**, *129*, 14500–14510.
(12) Coufal, D. E.; Blazyk, J. L.; Whittington, D. A.; Wu, W. W.; Rosenzweig, A. C.; Lippard, S. J. *Eur. J. Biochem.* **2000**, *267*, 2174–2185.
(13) Sazinsky, M. H.; Bard, J.; Di Donato, A.; Lippard, S. J. *J. Biol. Chem.* **2004**, *279*, 30600–30610.
(14) Liu, K. E.; Valentine, A. M.; Qiu, D.; Edmondson, D. E.; Appelman, E. H.; Spiro, T. G.; Lippard, S. J. *J. Am. Chem. Soc.* **1995**, *117*, 4997–4998.
(15) Lee, S.-K.; Lipscomb, J. D. *Biochemistry* **1999**, *38*, 4423–4432.
(16) Liu, K. E.; Wang, D.; Huynh, B. H.; Edmondson, D. E.; Salifoglou, A.; Lippard, S. J. *J. Am. Chem. Soc.* **1994**, *116*, 7465–7466.
(17) Broadwater, J. A.; Ai, J.; Loehr, T. M.; Sanders-Loehr, J.; Fox, B. G. *Biochemistry* **1998**, *37*, 14664–14671.
(18) Bollinger, J. M., Jr.; Krebs, C.; Vicol, A.; Chen, S.; Ley, B. A.; Edmondson, D. E.; Huynh, B. H. *J. Am. Chem. Soc.* **1998**, *120*, 1094–1095.
(19) Moënne-Loccoz, P.; Baldwin, J.; Ley, B. A.; Loehr, T. M.; Bollinger, J. M., Jr. *Biochemistry* **1998**, *37*, 14659–14663.
(20) Bailey, L. J.; McCoy, J. G.; Phillips, J.; George, N.; Fox, B. G. *Proc. Natl. Acad. Sci. U.S.A.* **2008**, *105*, 19194–19198.
(21) Cafaro, V.; Scognamiglio, R.; Viggiani, A.; Izzo, V.; Passaro, I.; Notomista, E.; Dal Piaz, F.; Amoresano, A.; Casbarra, A.; Pucci, P.; Di Donato, A. *Eur. J. Biochem.* **2002**, *269*, 5689–5699.
(22) Tinberg, C. E.; Song, W. J.; Izzo, V.; Lippard, S. J. Manuscript in preparation.
(23) Cafaro, V.; Notomista, E.; Capasso, P.; Di Donato, A. *Appl. Environ. Microbiol.* **2005**, *71*, 4736–4743.
(24) Liu, Y.; Nesheim, J. C.; Lee, S.-K.; Lipscomb, J. D. *J. Biol. Chem.* **1995**, *270*, 24662–24665.
(25) Murray, L. J.; García-Serres, R.; Naik, S.; Huynh, B. H.; Lippard, S. J. *J. Am. Chem. Soc.* **2006**, *128*, 7458–7459.
(26) Sjöberg, B.-M.; Karlsson, M.; Jörnvall, H. *J. Biol. Chem.* **1987**, *262*, 9736–9743.
(27) Pereira, A. S.; Small, W.; Krebs, C.; Tavares, P.; Edmondson, D. E.; Theil, E. C.; Huynh, B. H. *Biochemistry* **1998**, *37*, 9871–9876.
(28) Kim, K.; Lippard, S. J. *J. Am. Chem. Soc.* **1996**, *118*, 4914–4915.
(29) Yamashita, M.; Furutachi, H.; Tosha, T.; Fujinami, S.; Saito, W.; Maeda, Y.; Takahashi, K.; Tanaka, K.; Kitagawa, T.; Suzuki, M. *J. Am. Chem. Soc.* **2007**, *129*, 2–3.

JA9011782